

Fluid-fluid versus fluid-solid demixing in mixtures of parallel hard hypercubes

Luis Lafuente¹ and Yuri Martínez-Ratón²

¹ Departamento de Matemáticas, Escuela Superior de Ingeniería, Universidad de Cádiz, Calle Doctor Marañón 3, 11002 Cádiz, Spain.

E-mail: luis.molinero@uca.es

² Grupo Interdisciplinar de Sistemas Complejos (GISC), Departamento de Matemáticas, Escuela Politécnica Superior, Universidad Carlos III de Madrid, Avenida de la Universidad 30, 28911-Leganés, Madrid, Spain.

E-mail: yuri@math.uc3m.es

Abstract. It is well known that increase of the spatial dimensionality enhances the fluid-fluid demixing of a binary mixture of hard hyperspheres, i.e. the demixing occurs for lower mixture size asymmetry as compared to the three-dimensional case. However, according to simulations, in the latter dimension the fluid-fluid demixing is metastable with respect to the fluid-solid transition. According to the results obtained from approximations to the equation of state of hard hyperspheres in higher dimensions, the fluid-fluid demixing might become stable for high enough dimension. However, this conclusion is rather speculative since none of these works have taken into account the stability of the crystalline phase (by a minimization of a given density functional, by spinodal calculations or by MC simulations). Of course, the lack of results is justified by the difficulty of performing density functional calculations or simulations in high dimensions and, in particular, for highly asymmetric binary mixtures. In the present work, we will take advantage of a well tested theoretical tool, namely the fundamental measure density functional theory for parallel hard hypercubes (in the continuum and in the hypercubic lattice). With this, we have calculated the fluid-fluid and fluid-solid spinodals for different spatial dimensions. We have obtained, no matter what the dimensionality, the mixture size asymmetry or the polydispersity (included as a bimodal distribution function centered around the asymmetric edge-lengths), that the fluid-fluid critical point is always located above the fluid-solid spinodal. In conclusion, these results point to the existence of demixing between at least one solid phase rich in large particles and one fluid phase rich in small ones, preempting a fluid-fluid demixing, independently of the spatial dimension or the polydispersity.

PACS numbers: 64.75.Gh, 64.75.Cd, 64.60.De, 64.70.qd

Keywords: classical phase transitions (theory), phase diagrams (theory), monodisperse fluids, mixtures and polydisperse fluids, discrete fluid models

1. Introduction

Entropy-driven demixing was an active line of research since the 1990s. Several works had shown the presence of fluid-fluid (F-F) demixing in binary mixtures of hard anisotropic particles [1, 2, 3, 4, 5, 6]. The demixed phases can have different symmetries, with or without long range orientational order, the so called nematic or isotropic phases respectively. However, the simplest binary mixture of hard particles one can imagine, namely the hard sphere (HS) mixture, does not demix into two fluid phases even for high mixture size asymmetry. The first simulation study on the fluid-solid phase separation in the binary mixture of hard spheres [7] does not report any F-F demixing. However, they only consider mixtures with diameter ratios very close to one. More recent theoretical and simulation works on this system consider more asymmetric mixtures and for large enough asymmetry they have shown that the F-F demixing is metastable with respect to the fluid-solid (F-S) phase separation, with the crystalline phase rich in large spheres while the fluid phase is mostly populated by small spheres [8, 9]. In these works the F-F instability is taken into account in the computer simulations by approximating the effective hamiltonian through an explicit depletion potential approximation (integrating out the degrees of freedom of the small spheres). The same scenario occurs in binary mixtures of parallel hard cubes (PHC) with particles freely moving over space [10] or constrained on a lattice [11]. Note that although the cubes are anisotropic particles, the gain in the entropic volume after demixing can only be reached by changing the mixture composition or the density. As the cubes are parallel, the orientational entropy does not play any role here. In this sense the mixture of PHC is similar to the HS mixture. However, the effective depletion pair potential between two large solute particles immersed in a solvent of small particles is greater if the particles have cubic symmetry. As a matter of fact, this is why the scaled particle theory (SPT) applied to cubes predicts a metastable F-F demixing [10], while the same theory applied to HS does not.

In contrast to mixtures of additive HS, mixtures of non-additive HS can exhibit a stable F-F demixing as was shown by several authors both theoretically and by simulations [12]. This behavior can be perfectly understood by resorting to the following argument: when the interactions between different species are more repulsive (with a larger excluded volume) than those corresponding to the same species, the particles in the demixed configurations have a lower entropic volume and thus a greater configurational entropy (and consequently a lower free-energy).

The study of the hard hypersphere (HHS) one-component fluid has received great attention in recent years because certain questions that are ambiguous in 3D, e.g., jamming, crystallization, glass formation, find clearer answers when examined from a dimensional perspective. Also the poor knowledge of the lattice packing properties of HHS in high dimensions has led to works toward that direction [13]. Recent works have shown that the freezing of HHS is frustrated because configurations of spheres with simplex liquid ordering are very different from those corresponding to the periodic

lattice geometry [14]. Also calculations of the pair correlation functions $g_2(r)$ evince that the short-range ordering decreases appreciably with dimensions [15]. The frustration translates into higher free-energy barriers between the fluid and crystal states [14, 15] and thus the fluid has a greater propensity (than in three dimensions) to form a glass upon compression [15]. Both, simulations [14, 15, 16] and density functional calculations [17] have shown that the F-S transition occurs at lower packing fractions as the dimensionality increases and also that the character of this transition remains of first order. This does not mean that freezing is favoured when the dimensionality increases, since close packing is also reached at lower densities. Finally, the HHS fluid has been used as a test for different theoretical approximations of the structural properties of the fluid, comparing the direct correlation function $c(r)$ and the radial distribution function $g(r)$ obtained from these theories with those obtained by MC and MD computer simulations [18, 19, 20].

Returning to the demixing behavior of binary mixtures composed of particles interacting with hard-core potentials, we should say that the number of theoretical studies carried out in dimensions higher than three are very small, to our knowledge there is only one [21]. In this work the authors have shown that the F-F demixing of a binary mixture of HHS is favored as the dimensionality increases, i.e. the demixing shows up at lower mixture size asymmetry when the dimensionality increases. Notwithstanding, this is not conclusive enough to discard that one of the demixed phases could be unstable with respect to the freezing transition. The only way to settle this question is to involve the crystalline phase of a binary mixture in the theoretical or simulation studies, which obviously becomes a much more difficult task as compared to three dimensions.

The aim of the present work is to get some insights into what is the most likely scenario: F-F versus F-S demixing in a mixture of parallel hard hypercubes (PHHC). We have selected this system because the freezing of PHHC is much less affected by the geometric frustration present in HHS and thus the study is easier to carry out. For example, the simple hypercubic lattice is probably the most stable configuration of particles in a crystalline phase, and the same should occur in the crystalline phase of a binary mixture when small cubes occupy a very small fraction of the total volume. The other reason behind this selection is related to the theoretical tool we will apply to this study: the fundamental measure density functional theory developed for a mixture of PHHC defined on a lattice [22] or on the continuum [23]. As has already shown, the fundamental measure theory (FMT) applied to a HS fluid gives the most accurate results for the freezing transition as compared to other density functional theories [24]. Comparison between theory and simulations also confirms the high performance of this theory in predicting the equation of state of the crystalline phase of PHC [10]. Also, we have already shown that in three dimensions the F-F demixing is metastable with respect to the F-S demixing even for high mixture size asymmetry [10]. Simulations carried out on binary mixtures of parallel hard squares found strong clustering of large squares with crystalline structure in coexistence with a fluid of small squares [25] which would confirm this scenario in small dimensions. Note that this is in accordance with

SPT prediction for this system of a stable mixed phase with respect to the F-F demixing.

In the present paper we use FMT for PHHC to perform a F-S bifurcation analysis which together with the F-F spinodal calculations allow us to conclude that the F-F demixing is preempted by the freezing of at least one of the segregated phases (that is rich in large hypercubes). We show that this result holds up to the 9th dimension. For dimensions greater than 9 the third virial approximation is accurate enough and we can use it to show that the same scenario remains up to dimension 25. For higher dimensions, we have carried out an asymptotic analysis of the second virial approach (which becomes exact in the limit of infinite dimension) and the conclusions do not change: the F-S demixing preempts the F-F demixing. Finally, we have included polydispersity in the edge length of the PHHC by means of a bimodal distribution function and again we find the same scenario.

The paper is organized as follows. In Sec. 2 we present the expressions for the direct correlation functions of a mixture of PHHC as obtained from the FMT defined on a lattice and on the continuum. These functions allow us to perform an F-S bifurcation analysis and to calculate the F-F demixing spinodals. In Sec. 3 we show the results from these calculations. This section is divided into three parts: in Sec. 3.1 we present the results from the F-S bifurcation analysis of the one-component fluid of PHHC as a function of dimensionality; Sec. 3.2 is devoted to a detailed study of the demixing transitions as a function of mixture size asymmetry and dimensionality; and finally in Sec. 3.3 we present the results from the bifurcation analysis of a bimodal polydisperse mixture of PHHC. In Sec. 4 we carry out an asymptotic analysis (for large dimensions) of the second virial approximation which allows us to conclude that at infinite dimension the F-F demixing is metastable with respect to the F-S demixing. The conclusions are drawn in Sec. 5 and theoretical details of the bifurcation analysis are relegated to an appendix.

2. Model

The model consists of a binary mixture of PHHC embedded in dimension n with species $i = 1, 2$ having an edge length equal to σ_i . We define mixture size asymmetry by the coefficient $\kappa = \sigma_2/\sigma_1 \geq 1$. The mixture is fully characterized by the density profiles $\rho_i(\mathbf{r})$ where the vector $\mathbf{r} \equiv (x_1, x_2, \dots, x_n)$ denotes the position of the center of mass of a particle in the n -dimensional space. If the particle positions are constrained to be on a simple hypercubic lattice the variables x_i are set equal to $i \in \mathbb{Z}$ (i.e. we are using the lattice mesh size as the unit of length). Note that when the lattice mesh size goes to zero, the lattice model goes to the continuum model, therefore in the lattice model we have chosen $\sigma_2 = 2$ in order to emphasize its discrete nature. We will use the density functional (DF) based on the FMT obtained by us already on a lattice [22] and on the continuum [23]. We refer the reader to those references for a detailed description of the way to obtain the DF from the free-energy density of a so called zero-dimensional cavity, which can accommodate one particle at the most. For a more general reference

on the theory see Refs. [26, 27].

From the DF we can obtain the Fourier transform of the direct correlation functions which are the only expressions we need to compute the F-F and F-S spinodals corresponding to the F-F or F-S demixing transitions. From these, we can analyze the relative stability between F-F and F-S transitions.

2.1. Direct correlation functions following the FMT for PHHC

As we have already shown in [22, 23] the excess part of the free-energy DF corresponding to a mixture of PHHC in dimension n , $\beta\mathcal{F}_{\text{ex}}[\{\rho_i\}]$, can be obtained from the excess free energy of a zero-dimensional cavity

$$\Phi_0(\eta) = \eta + (1 - \eta) \ln(1 - \eta), \quad (1)$$

η being the packing fraction of the cavity.

In particular, for the continuum c -component mixture of parallel hard hyperparallelepipeds we have

$$\beta\mathcal{F}_{\text{ex}}[\{\rho_i\}] = \int d\mathbf{r} \Phi_n(\mathbf{r}),$$

$$\Phi_n(\mathbf{r}) \equiv \left(\prod_{l=1}^n \sum_{i=1}^c \frac{\partial}{\partial \sigma_i^{(l)}} \right) \Phi_0(\eta(\mathbf{r})), \quad (2)$$

$$\eta(\mathbf{r}) = \sum_{i=1}^c \int_{x_1 - \sigma_i^{(1)}/2}^{x_1 + \sigma_i^{(1)}/2} dx'_1 \dots \int_{x_n - \sigma_i^{(n)}/2}^{x_n + \sigma_i^{(n)}/2} dx'_n \rho_i(\mathbf{r}'), \quad (3)$$

$\eta(\mathbf{r})$ being the local packing fraction of a maximal zero-dimensional cavity centered at \mathbf{r} and $\sigma_i^{(l)}$ being the edge length of component i in the l spatial direction. The analogous expressions for the discrete case are

$$\beta\mathcal{F}_{\text{ex}}[\{\rho_i\}] = \sum_{\mathbf{r} \in \mathbb{Z}^n} \Phi_n(\mathbf{r}),$$

$$\Phi_n(\mathbf{r}) \equiv \left(\prod_{l=1}^n \Delta_{k_l} \right) \Phi_0(\eta^{(\mathbf{k})}(\mathbf{r})), \quad \Delta_k f(k) \equiv f(1) - f(0), \quad (4)$$

$$\eta^{(\mathbf{k})}(\mathbf{r}) = \sum_{i=1}^c \sum_{x'_1 = x_1 - \sigma_i^{(1)}/2 + 1 - k_1}^{x_1 + \sigma_i^{(1)}/2 - 1} \dots \sum_{x'_n = x_n - \sigma_i^{(n)}/2 + 1 - k_n}^{x_n + \sigma_i^{(n)}/2 - 1} \rho_i(\mathbf{r}'), \quad \mathbf{k} \in \{0, 1\}^n, \quad (5)$$

$\eta^{(\mathbf{k})}(\mathbf{r})$ being the packing fraction of a zero-dimensional cavity around \mathbf{r} . For a connection between the difference operator in equation (4) and the Möbius inversion formula, the reader is referred to [26].

Using Eqs. (2) and (4), we can calculate the direct correlation functions defined through the second functional derivative, $c_{ij}^{(n)}(\mathbf{r}_{12}) = -\delta^2 \beta\mathcal{F}_{\text{ex}}^{(n)} / \delta \rho_i(\mathbf{r}_1) \delta \rho_j(\mathbf{r}_2)$, evaluated at uniform density profiles $\rho_i(\mathbf{r}) = \rho_i$. If we calculate the Fourier transforms of these functions, evaluate them at the wave vector $\mathbf{q} = q(1, 0, \dots, 0)$ and take $\sigma_i^{(k)} = \sigma_i$ for any

k , in the continuum we obtain

$$\begin{aligned}
 -\hat{c}_{ij}^{(n)}(q) &= \sum_{k=0}^{n-1} C_k^{n-1} (\sigma_i \sigma_j)^k \sigma_{ij}^{n-1-k} \\
 &\quad \times [\zeta_k \sigma_{ij} j_1(q\sigma_{ij}/2) + \zeta_{k+1} \sigma_i \sigma_j j_1(q\sigma_i/2) j_1(q\sigma_j/2)], \quad (6)
 \end{aligned}$$

with $\sigma_{ij} = \sigma_i + \sigma_j$, $C_k^n = n!/k!(n-k)!$ the usual combinatorial coefficients and $j_1(x)$ the spherical Bessel function of first order. The functions $\zeta_k(\xi_{n-k}, \dots, \xi_n)$ with $k = 0, \dots, n$ can be obtained recurrently from $\zeta_0(\xi_n) = 1/(1 - \xi_n)$ using the following relations

$$\zeta_{k+1}(\xi_{n-k-1}, \dots, \xi_n) = \sum_{i=0}^k \xi_{n-i-1} \frac{\partial \zeta_k(\xi_{n-k}, \dots, \xi_n)}{\partial \xi_{n-i}}, \quad k = 0, \dots, n-1 \quad (7)$$

where we have defined $\xi_k = \sum_i \rho_i \sigma_i^k$. Note that the packing fraction η is just equal to ξ_n . For the lattice version we have

$$\begin{aligned}
 -\hat{c}_{ij}^{(n)}(q) &= \sum_{k=0}^{n-1} C_k^{n-1} (-1)^{n-k} (\sigma_i \sigma_j)^k [(\sigma_i - 1)(\sigma_j - 1)]^{n-k-1} \frac{1}{\sin^2(q/2)} \\
 &\quad \times \left[\frac{\sin(q\sigma_i/2) \sin(q\sigma_j/2)}{1 - \eta_{k+1}} - \frac{\sin(q(\sigma_i - 1)/2) \sin(q(\sigma_j - 1)/2)}{1 - \eta_k} \right], \quad (8)
 \end{aligned}$$

where we have defined $\eta_k = \sum_i \rho_i \sigma_i^k (\sigma_i - 1)^{n-k}$ for $k = 0, 1, \dots, n$, which is the uniform version of $\eta^{(\mathbf{k})}(\mathbf{r})$ with $k \equiv k_1 + \dots + k_n$.

The fluid pressure of the mixture in the continuum is related to the function $\zeta_n(\xi_0, \dots, \xi_n)$ through the relation $\zeta_n = \partial \beta p / \partial \xi_n$. The lattice version give us the following expression for the pressure

$$\beta p = - \sum_{k=0}^n C_k^n (-1)^{n-k} \ln(1 - \eta_k). \quad (9)$$

We should note that the expressions (6) and (8) in the low density limit $\rho_i \rightarrow 0$ recover the exact second and third virial approximations.

2.2. F-F and F-S spinodals

The packing fraction η (note that $\eta = \xi_n$ in the continuum and $\eta = \eta_n$ in the lattice) and the wave number q at the F-S transition of the binary mixture can be calculated from the singularity of the matrix with coefficients defined through the partial structure factors

$$S_{ij}(q, \eta) = \delta_{ij} - \rho \sqrt{x_i x_j} \hat{c}_{ij}^{(n)}(q), \quad (10)$$

with $x_i = \rho_i / \rho$ the mixture composition and $\rho = \sum_i \rho_i$ the total density. The singularity condition gives us, at a fixed composition x_1 ($x_2 = 1 - x_1$),

$$\begin{aligned}
 \Delta(q, \eta, x_1) &\equiv \det \begin{pmatrix} 1 - \rho x_1 \hat{c}_{11}^{(n)}(q) & -\rho \sqrt{x_1 x_2} \hat{c}_{12}^{(n)}(q) \\ -\rho \sqrt{x_1 x_2} \hat{c}_{12}^{(n)}(q) & 1 - \rho x_2 \hat{c}_{22}^{(n)}(q) \end{pmatrix} \\
 &= \left(1 - \rho_1 \hat{c}_{11}^{(n)}(q)\right) \left(1 - \rho_2 \hat{c}_{22}^{(n)}(q)\right) - \rho_1 \rho_2 \left(\hat{c}_{12}^{(n)}(q)\right)^2 = 0. \quad (11)
 \end{aligned}$$

Now, we should look for the lowest value of η that satisfied this equation. If we take into account that $\Delta(\eta, q, x_1) = 0$ defines a function $\eta_{\text{sing}}(q, x_1)$, in order to find the values $\eta_{\text{bif}}(x_1)$ and q_{bif} at the F-S transition we need to solve

$$\begin{aligned}\eta_{\text{bif}}(x_1) &= \min_{q>0} \eta_{\text{sing}}(q, x_1), \\ q_{\text{bif}} &= \arg \min_{q>0} \eta_{\text{sing}}(q, x_1).\end{aligned}\tag{12}$$

In the continuum this is equivalent to the set of equations

$$\Delta(q, \eta, x_1) = \frac{\partial \Delta(q, \eta, x_1)}{\partial q} = 0,\tag{13}$$

In the lattice version, due to the discrete nature of q (in units of the lattice mesh size) we do not have the second equality in (13). Finally, in both cases the F-F spinodal can be calculated from the condition $\Delta(0, \eta, x_1) = 0$.

3. Results

This section is divided into three parts. The first one is devoted to showing the performance of our theory concerning the calculation of the F-S transition of a one-component fluid of PHHC as a function of dimensionality n . In the second part we analyze the relative stability between the F-F and F-S demixing, again as a function of n , of (i) a binary mixture of PHHC and of (ii) a bimodal polydisperse fluid. For the former system, we have carried out the analysis both in the continuum and in the lattice cases, while for the latter only the continuum system is studied. The last part of the section is devoted to the study of the binary mixture phase behavior at infinite dimension, by means of an asymptotic analysis.

3.1. One component fluid

As we have already shown using both versions of the FMT, the continuum parallel hard cube fluid in dimension three exhibits a second order F-S transition where the cubes crystallize in a simple cubic lattice [23]; in the lattice version [22] the system shows a second order transition where the structure of the ordered phase depends on the size of the cubes (from smectic for the smallest cubes possible to solid for larger sizes). Herein we will be referring to F-S demixing for both the continuum and lattice model, but we ask the reader to take into account that in the discrete case the structure of the ordered phase could be different from a solid. In the continuum the same behavior was also predicted from simulations [28, 29, 30]. Although the character (second order vs. first order), and the symmetry of the crystalline phase were adequately predicted from FMT as compared to MC simulation results, the precise location of the transition point is underestimated by the theory [10]. This discrepancy is explained by noting that the uniform limit of the FMT recovers the SPT and, therefore, the fluid phase predicted by FMT inherits all its defects. While all the virial coefficients predicted by SPT are positive, it is known that this is not the real case [31, 32] where the presence of negative

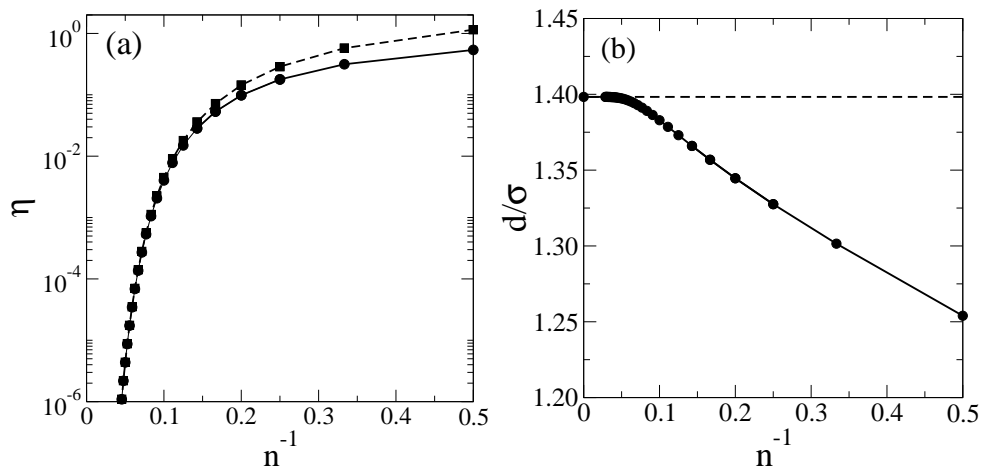


Figure 1. Packing fraction η (a) and period of the crystalline phase d/σ (b) at bifurcation as a function of the dimensionality n .

coefficients results in a poor convergence of the virial expansions. As a consequence, although FMT recovers the low-density limit, the equation of state for the fluid near the transition point is not very accurate. Notwithstanding, because of the dimensional crossover property of the FMT DFs, the predictive power of FMT is greatly enhanced when the packing fraction of the crystalline phase is high enough. Actually, for packing fractions $\eta \geq 0.5$ the comparison between theory and simulations is fairly good [10]. Finally, for dimensions higher than three we should remark that there is a rigorous result that shows that at infinite dimension the PHHC fluid exhibits a second order phase transition to a crystalline phase with a simple hypercubic symmetry [33].

We calculate here the F-S transition of the continuum PHHC as a function of the dimensionality using a bifurcation analysis, i.e. by solving the equations (13) in the one-component limit to find the packing fraction η_{bif} and the period in units of the edge length d/σ at the transition point (note that d is related to q_{bif} as $d/\sigma = 2\pi/q_{\text{bif}}$). These values are plotted in figures 1 (a) and (b), respectively. As is already known, the second virial approximation becomes exact in the limit $n \rightarrow \infty$. Here, the packing fraction at the transition scales with n as $\eta \sim 2^{-n}$. With the aim of comparison, we have also plotted in figure 1 the results from this approach. As we can see from the figure, the packing fraction η_{bif} and the period d/σ obtained from both FMT and second virial approximations are very similar when $n \sim 10$. Therefore, it should be expected that around this value of the dimension and for higher ones FMT predictions should not differ too much from those obtained by means of a virial expansion. This supports our approach in the next subsections where we have analyzed the binary mixture stability using FMT only up to $n = 9$ and from there to $n = 25$ we have used the third virial expansion instead, and we have concluded with an asymptotic analysis of the second virial expansion, which should be accurate enough for higher dimensions.

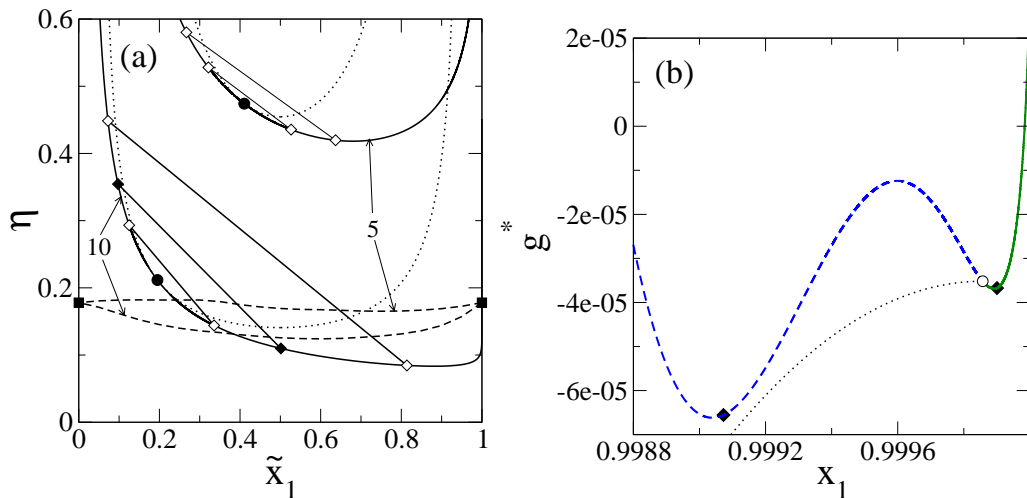


Figure 2. (a) F-F (dotted) and F-S (dashed) spinodals in the packing fraction-composition plane for a binary mixture of PHHC in dimension four and mixture asymmetries equal to $\kappa = 5$ and $\kappa = 10$. The coexistence F-F binodals are also plotted with solid lines. The solid circles indicate the position of the critical points while the diamonds joined by straight lines indicate some examples of coexisting fluid phases (note that one or both of them are metastable with respect to the freezing transition). The solid squares indicate the F-S transition of the pure one-component fluid. (b) The Gibbs free energy per particle in reduced units minus a straight line (to make the coexistence more visible) $g^* = \beta G/N - 7.4962 - 1273.2x_1$ as a function of the molar fraction of the small component. The mixture size asymmetry is $\kappa = 10$ and the pressure is fixed to $\beta p \sigma_1^3 = 939.49$ [coinciding with that corresponding to the coexistence points labeled with filled diamonds in (a)]. The filled diamonds indicate the F-F coexisting points while the open circle indicates the F-S bifurcation point. To the left of this point the fluid branch (with the dashed line) is unstable with respect to the solid branch sketched (not calculated) with the dotted line.

3.2. F-F versus F-S demixing in binary mixtures of PHHC

In this section, we will analyze the phase behavior of the binary mixture of PHHC as a function of the dimensionality. As was already shown in dimension three, the F-F demixing is always unstable with respect to the F-S demixing in which a crystalline phase preferentially populated by large cubes coexists with a fluid phase rich in small cubes [10]. The uniform mixture becomes unstable with respect to the F-F demixing for a mixture size asymmetry $\kappa = 5 + \sqrt{24} \approx 10$ in the continuum and $\kappa = 13$ in the lattice. However, the position of the critical point of the F-F spinodal curve in the packing fraction-composition plane is always located above the F-S spinodal curve, the latter computed from the set of equations (12). This is equivalent to saying that at least one of the coexisting uniform phases is unstable with respect to the freezing transition.

We have found the same scenario for higher dimensions. The main differences are only quantitative and can be summarized as follows: the lowest mixture size asymmetry at which the F-F phase separation shows up (see table 1) decreases dramatically with the dimensionality and the same happens with the packing-fraction value at the critical

n	3	4	5	6	7
κ_{cont}^*	9.90	3.73	2.54	2.09	1.87
κ_{latt}^*	13	5	3	3	2

Table 1. Critical aspect ratio κ^* for which the F-F demixing appears for the first time in the continuum and lattice models.

point. Thus the demixing transition is enhanced with n . On the other hand, the packing-fraction values at the F-S spinodal also decrease with n , and although they get closer to the F-F spinodal in the neighborhood of the critical point, they remain always below it. This behavior is present even for high values of the mixture size asymmetry. It is worth noting that κ^* for the continuum model decreases as the inverse of the dimension; actually from the values shown in table 1 we have found that κ^* follows very accurately the law $\kappa^* = 1 + a/(n - b)$ where $a = 3.809$ and $b = 2.566$. The conclusion is that, no matter what the dimension or the mixture size asymmetry, the most probable scenario is the presence of demixing between a fluid phase rich in small cubes and a crystalline phase mostly populated by large ones. This scenario is illustrated in figure 2 where we have plotted both spinodals (F-F and F-S) and the F-F coexistence binodals obtained from the continuous model of PHHC in dimension four and asymmetries fixed to $\kappa = 5$ and $\kappa = 10$. Note that we have used to represent the composition of the mixture the volume composition \tilde{x}_1 , which is related to the molar fraction as $\tilde{x}_i = \sigma_i^n x_i / \langle \sigma^n \rangle$, where $\langle \sigma^n \rangle \equiv \sum_i \sigma_i^n x_i$. As we can see from the figure, the critical point in the F-F spinodal (\tilde{x}_1^c, η^c) is located above the F-S spinodal, therefore at least one of coexisting fluid phases is unstable with respect to the freezing transition. This scenario is illustrated in figure 2(b), where we plot the Gibbs free-energy per particle as a function of the molar fraction of small cubes x_1 for a fixed value of the fluid pressure (note the difference between \tilde{x}_1 and x_1 due to the huge difference in volume between the large and small cubes). From the left of the F-S bifurcation point (open circle), the fluid branch is usually located above the solid branch which is sketched with a non-convex curve. From our earlier calculations in $n = 3$ the convexity of the solid branch is usually recovered when the volume fraction of big cubes is near unity. As we have already shown in [34] the infinite mixture size asymmetry limit corresponds to a one-component fluid of sticky cubes. For this case, at any fixed solvent fugacity, the coexistence is between an infinite dilute vapor phase and a close-packed crystal. When we include a small amount of polydispersity in the edge length of the large cubes the convexity of the solid branch is recovered at high packing fractions, and the coexistence is now between a highly dense crystal and a vapor phase. We expect a similar behavior for a highly asymmetric mixture.

In figure 3, we show the phase behavior of both continuum (figures (a) and (b)) and lattice (figures (c) and (d)) PHHC for $n = 4$ and $n = 5$ for a large set of mixture size asymmetries, some of them being as high as $\kappa = 100$. It is remarkable that even for very high values of κ the behavior is the same as that described above: the F-S demixing is the most likely scenario.

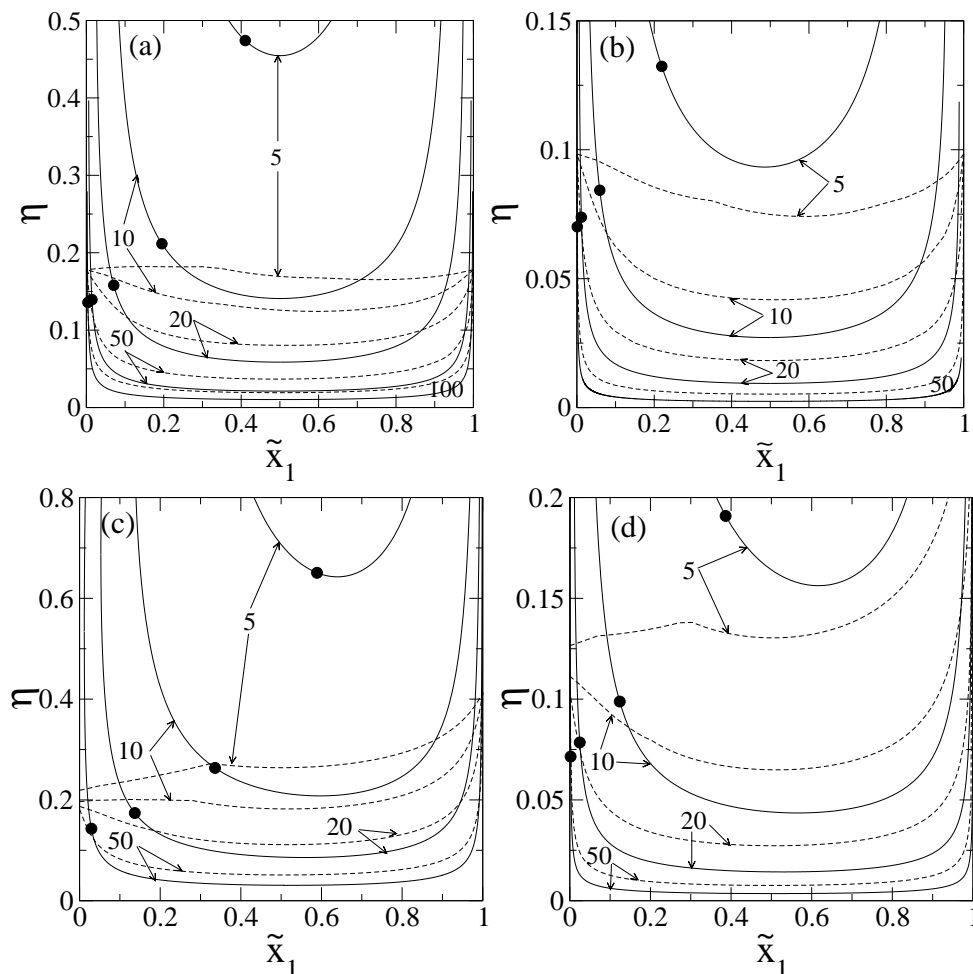


Figure 3. Phase behavior of a binary mixture of PHHC in the continuum [(a) and (b)] and in the lattice [(c) and (d)] for dimensions 4 [(a) and (c)] and 5 [(b) and (d)]. The solid and dashed lines represent the F-F and F-S spinodals for different values of the mixture asymmetry κ (correspondingly labeled in the figure). The filled circles indicate the locations of the F-F critical points.

This trend can be better appreciated in figures 4(a) and (b) (for the continuous model) and (c) and (d) (for the lattice model), where we plot the coefficient $R_n \equiv (\eta^c - \eta_{\text{bif}}(x_1^c))/\eta_{\text{bif}}(x_1^c)$ which measures the relative distance between both spinodals at the F-F critical point as a function of n . As we can see from the figure, this coefficient decreases with n up to a certain dimension (the position of the minimum) which depends on κ , and further increases with n diverging at $n \rightarrow \infty$ (this will be shown by means of the asymptotic analysis presented in section 4). In these figures are also shown the period d/σ_2 of the crystalline mixed phase with $\tilde{x}_1 = \tilde{x}_1^c$ calculated at bifurcation as a function of n , and the period of the one-component crystal. In general, for low dimensions the crystalline phase of large cubes becomes more packed by adding an small amount of small cubes, an effect clearly related with the entropic depletion forces.

Using the third virial approximation [equations (6) and (8) up to first order in

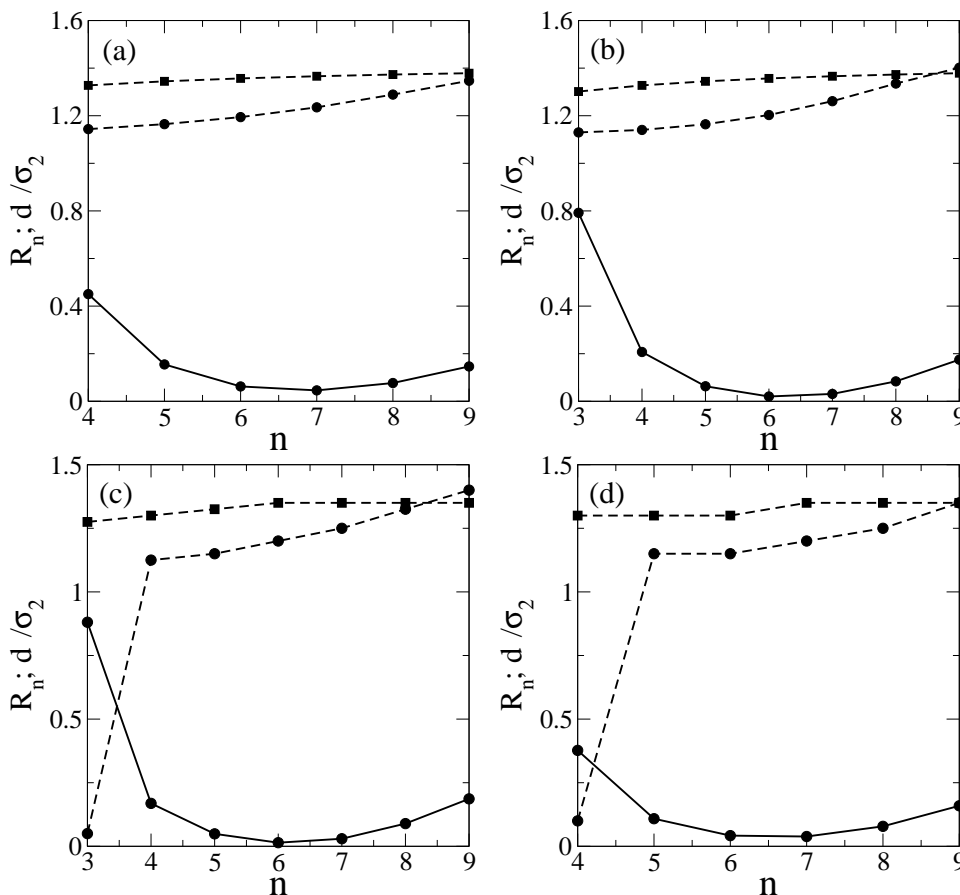


Figure 4. The coefficient R_n (solid line) and the lattice periods d/σ_2 corresponding to the crystalline mixed phase (the circles joined with dashed line) and to the one-component crystal (squares joined with dashed line) as a function of n as obtained from the continuum [(a) and (b)] and the lattice [(c) and (d)] models. The values for the mixture asymmetries are $\kappa = 10$ [(a) and (c)] and $\kappa = 20$ [(b) and (d)].

density] we have extended the spinodal calculations up to dimension 25. In figure (5) we plot the packing fractions of the F-F critical point and of the F-S transition at \tilde{x}_1^c as a function of n in both the continuum and the lattice models. Again, we find the expected behavior: the freezing preempts the F-F demixing.

3.3. Effect of polydispersity on the F-F and F-S demixing

We have also studied the effect that the polydispersity has on the demixing behavior of PHHC. We have relegated to the appendix the formalism that leads to the main equations for the F-F and F-S spinodals. If we introduce polydispersity in the cube-edge lengths around their mean values $\sigma_1 = 1$ and $\sigma_2 = 50$ (i.e. following a bimodal distribution function) for $n = 3$ and $\sigma_2 = 20$ for $n = 4$, we find that the crystalline phase destabilizes with respect to the fluid phase as the polydispersity increases. However, although the F-F critical point gets closer to the F-S spinodal it is still located above it, even for large polydispersities (see figures 6 (a) and (b)).

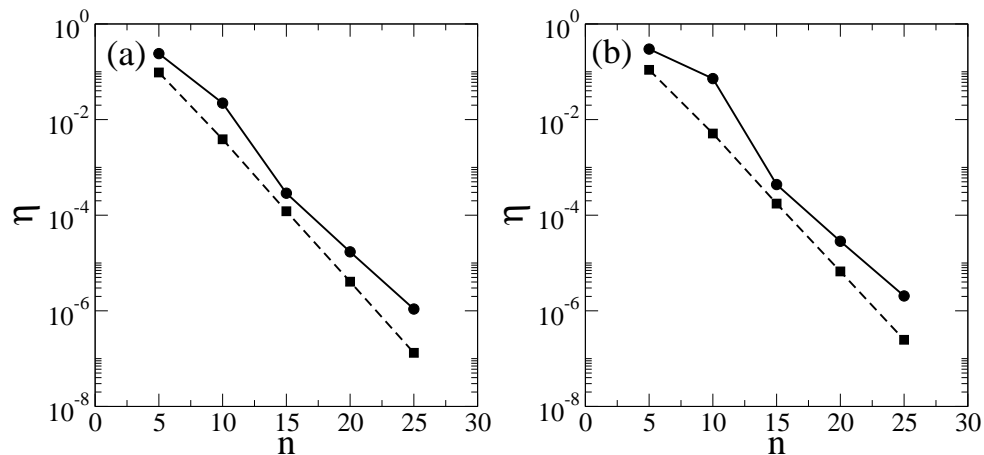


Figure 5. The packing fractions corresponding to the the F-F critical point and to the the F-S transition at \tilde{x}_1^c as a function of dimensionality following the third virial approximation as obtained from the continuum (a) and lattice (b) models.

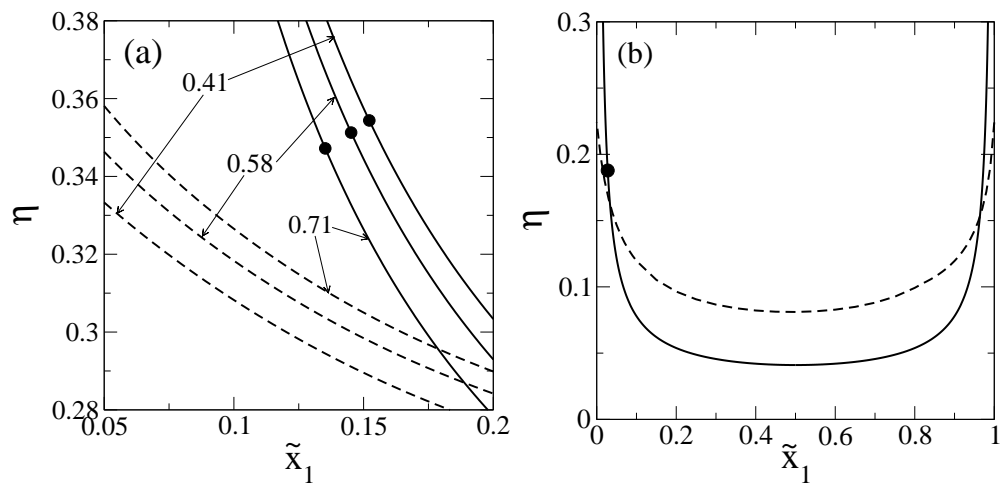


Figure 6. (a) F-F and F-S spinodals of PHHC in dimension three around the F-F critical point for different values of the polydisperse coefficient r as labeled in the figure. (b) The whole spinodals in dimension four at polydispersity $r = 0.577$. The mixture size asymmetry is fixed to $\kappa = 50$ in (a) and $\kappa = 20$ in (b). The circles specify the position of the critical points.

4. Asymptotic analysis

In this section we will carry out the asymptotic analysis for the functions $\eta^c(n)$ and $\tilde{x}_1^c(n)$ corresponding to the position of the F-F critical point as a function of dimensionality when $n \rightarrow \infty$. For this, we will use the second virial approach, as it becomes exact at this limit. The aim of the analysis is to find the relative position of the F-F critical point with respect to the F-S transition at large dimensions. In order to do that, we will use the asymptotic expressions for the F-F critical point to evaluate $\Delta(q_{\min}, \eta^c, x_1^c)$ (with q_{\min} the position of the absolute minimum of $\Delta(q, \eta^c, x_1^c)$ as a function of q). Note that if this quantity is negative, this means that the F-S transition is below the F-F

critical point. For the sake of simplicity, we will restrict this analysis to the continuum model. In the lattice case, the expressions become too cumbersome, but qualitatively there is no difference with the continuum model, so we have preferred not to include it in this paper.

The expression for the direct correlation functions $\hat{c}_{ij}^{(n)}(q)$ in the second virial approximation can be obtained from equation (6) as a Taylor expansion of zeroth order in the densities. In this approximation, the pressure can be cast as

$$\beta p = \rho + \frac{1}{2} \sum_{i,j} \rho_i \rho_j \sigma_{ij}^n. \quad (14)$$

In the following, we will use the volume composition \tilde{x}_i and the scaled packing fraction $\eta_0 \equiv \eta 2^n$ as the adequate variables to evaluate βp and $\Delta(q, \eta, x_1)$ when $n \gg 1$. In these new variables their expressions become

$$p^*(\eta_0, \tilde{x}_1) \equiv \beta p (2\sigma_1)^n = \eta_0 \left(\tilde{x}_1 + \frac{\tilde{x}_2}{\kappa^n} \right) + \frac{\eta_0^2}{2} \left[\tilde{x}_1^2 + \frac{\tilde{x}_2^2}{\kappa^n} + 2\tilde{x}_1 \tilde{x}_2 \left(\frac{1 + \kappa^{-1}}{2} \right)^n \right], \quad (15)$$

for the pressure and

$$\begin{aligned} \Delta(q, \eta_0, \tilde{x}_1) &= 1 + \tilde{x}_1 \eta_0 j_1(q\sigma_1) + \tilde{x}_2 \eta_0 j_1(q\sigma_2) + \tilde{x}_1 \tilde{x}_2 \eta_0^2 \\ &\quad \times \left[j_1(q\sigma_1) j_1(q\sigma_2) - \left(\frac{\kappa + \kappa^{-1} + 2}{4} \right)^n j_1^2(q\sigma_{12}/2) \right]. \end{aligned}$$

Note that $\tilde{x}_2 = 1 - \tilde{x}_1$. The above expression evaluated at $q = 0$ gives

$$\Delta(0, \eta_0, \tilde{x}_1) = 1 + \eta_0 - \tilde{x}_1 \tilde{x}_2 \delta_n \eta_0^2, \quad (16)$$

where we have defined the coefficient $\delta_n \equiv \kappa^{-n}[(\kappa + 1)/2]^{2n} - 1$. The equation $\Delta(0, \eta_0, \tilde{x}_1) = 0$ defines the F-F spinodal:

$$\eta_0^{\text{FF}}(\tilde{x}_1) = \frac{1 + \sqrt{1 + 4\delta_n \tilde{x}_1 \tilde{x}_2}}{2\tilde{x}_1 \tilde{x}_2 \delta_n}. \quad (17)$$

The critical point can be found as the value of \tilde{x}_1 at which $dp^*(\eta_0^{\text{FF}}, \tilde{x}_1)/d\tilde{x}_1 = 0$. When $n \rightarrow \infty$, the composition at the critical point \tilde{x}_1^c goes to zero (and therefore $\tilde{x}_2^c \asymp 1$); taking this into account and using the new variables $s_n \equiv \sqrt{1 + 4\delta_n \tilde{x}_1} - 1$ and $\tau_n \equiv \delta_n/\kappa^n$ we have

$$\frac{dp^*}{d\tilde{x}_1} \asymp \frac{2 + s_n}{2s_n^2(1 + s_n)} [s_n^3 - 4\sqrt{\tau_n}(1 + \sqrt{\tau_n})s_n - 8\tau_n], \quad (n \rightarrow \infty). \quad (18)$$

The asymptotic solution of $dp^*(\eta_0^{\text{FF}}, \tilde{x}_1)/d\tilde{x}_1 = 0$ with respect to s_n gives us $s_n \asymp \sqrt{\tau_n} + \sqrt{4\sqrt{\tau_n} + \tau_n}$ and then, at the F-F critical point,

$$\tilde{x}_1^c(n) \asymp (2\delta_n)^{-1} \left[3\sqrt{\tau_n} + \tau_n + (1 + \sqrt{\tau_n})\sqrt{4\sqrt{\tau_n} + \tau_n} \right], \quad (n \rightarrow \infty), \quad (19)$$

and from equation (17)

$$\eta_0^c(n) \asymp \tau_n^{-1/4} \sqrt{1 + \frac{\sqrt{\tau_n}}{4}} - \frac{1}{2}, \quad (n \rightarrow \infty). \quad (20)$$

From here we have that the leading terms in the asymptotic behavior at the F-F critical point are $\tilde{x}_1^c(n) \asymp [2\sqrt{2\kappa}/(\kappa + 1)^{3/2}]^n$ and $\eta_0^c(n) \asymp [2/(1 + \kappa^{-1})]^{n/2}$, respectively. Note

that although $\eta_0 \rightarrow \infty$ when $n \rightarrow \infty$ the packing fraction $\eta = 2^{-n}\eta_0$ goes to zero when $n \rightarrow \infty$.

The function $\Delta(q, \eta_0^c, \tilde{x}_1^c)$ is asymptotically

$$\Delta(q, \eta_0^c, \tilde{x}_1^c) \simeq 1 - j_1^2(q\sigma_{12}/2) + \eta_0^c [j_1(q\sigma_2) - j_1^2(q\sigma_{12}/2)], \quad (n \rightarrow \infty). \quad (21)$$

When $n \rightarrow \infty$, $\eta_0^c \rightarrow \infty$, and the dominant contribution to $\Delta(q, \eta_0^c, \tilde{x}_1^c)$ is just the term proportional to η_0^c in equation (21) which for $\kappa \gg 1$ has its absolute minimum at $q_{\min}\sigma_2 = 3.506$ with the value $\Delta(q_{\min}, \eta_0^c, \tilde{x}_1^c) = -0.416\eta_0^c$. This negative value implies that the mixture with composition and packing fraction corresponding to the F-F critical point is unstable with respect to the F-S transition. Thus, the F-F demixing is unstable with respect to the F-S demixing.

5. Conclusions

In the present work we have made the first attempt to answer to the question about how the dimensionality and mixture size asymmetry affect the relative stability of the F-F demixing of PHHC against the F-S phase separation, based on the bifurcation analysis for the latter transition. Although the results presented here strongly suggest the F-S demixing as the most likely scenario independently of the dimensionality and of the mixture size asymmetry, the final confirmation of this phase behavior can be given only after carrying out MC simulations or DFT coexistence calculations on this system. Both tasks become much more difficult as the mixture size asymmetry and dimensionality increase. The main difficulty in performing MC simulations consists of the high probability of overlapping many small cubes when a given large cube is moved by a MC step. Thus a more sophisticated simulation scheme like a cluster movement algorithm is required to carry out these simulations. Even using these schemes, the increase of spatial dimensionality (apart from the high mixture asymmetry) constitutes an additional complication due to the huge increase in the number of particles necessary to perform a simulation with a reliable statistics. Instead of performing an MC simulation on the binary mixture, it is possible to map the mixture onto an effective one-component fluid with particles interacting via an effective depletion potential which can be previously calculated using the formalism described in [8]. Although this mapping is approximate it should work very well for very asymmetric mixtures.

The extrapolation of this result to the HHS mixture or other additive hard mixtures should be made with some caution. The elevated barrier for freezing in higher dimensions might allow for the metastable F-F separation to be observed and particularly long lived. Also, as we have pointed out in section 1, the freezing transition in HHS becomes more frustrated with dimensionality. Thus it might possibly occur that at some dimension this frustration makes the F-F demixing the stable one. To elucidate this question we should wait for future works which we hope will have been motivated by the present one.

Acknowledgements

We acknowledge support from the Dirección General de Universidades e Investigación of the Comunidad de Madrid (Spain), under the R&D Programmes of activities MODELICO-CM/S2009ESP-1691 and to the Ministerio de Educación y Ciencia of Spain under the grants MOSAICO and FIS2010-22047-C05-C04

Appendix A. Polydisperse PHHC

In this appendix, we present the formalism used to prove that the transition to the crystalline phase preempts the F-F demixing even in polydisperse mixtures of PHHC. For this purpose we select a bimodal length distribution function as

$$h(\sigma) = xh_0(\sigma/\sigma_1) + (1-x)h_0(\sigma/\sigma_2), \quad (\text{A.1})$$

where $0 \leq x \leq 1$ is the polydisperse composition variable, and we use for $h_0(\sigma/\sigma_i)$ the normalized to unity Schultz distribution function with mean values fixed to σ_i ($i = 1, 2$):

$$h_0(\sigma/\sigma_i) = \frac{(\nu+1)^{\nu+1}}{\sigma_i \Gamma(\nu+1)} \left(\frac{\sigma}{\sigma_i}\right)^\nu \exp[-(\nu+1)\sigma/\sigma_i], \quad (\text{A.2})$$

where $\Gamma(x)$ is the Gamma function and ν controls the width of both peaks located in the neighborhood of σ_i and related with the polydisperse coefficient r of the distribution function $h_0(\sigma)$ as $r = \sqrt{\langle \sigma^2 \rangle_{h_0(\sigma)} / \langle \sigma \rangle_{h_0(\sigma)}^2} - 1 = 1/\sqrt{\nu+1}$. The moments of $h(\sigma)$ can be calculated as

$$\langle \sigma^\alpha \rangle_{h(\sigma)} \equiv \int_0^\infty d\sigma \sigma^\alpha h(\sigma) = \frac{\Gamma(\nu+\alpha+1)}{(\nu+1)^\alpha \Gamma(\nu+1)} (x\sigma_1^\alpha + (1-x)\sigma_2^\alpha). \quad (\text{A.3})$$

Near and above the F-S bifurcation point the density profile of a polydisperse mixture can be approximated as $\rho(\mathbf{r}, \sigma) \approx \rho_0(\sigma) + \epsilon(\mathbf{r}, \sigma)$, where $\rho_0(\sigma) = \rho_0 h(\sigma)$ is the density distribution corresponding to the uniform parent phase (with ρ_0 its number density) at bifurcation and $\epsilon(\mathbf{r}, \sigma)$ is a small non-uniform perturbation. The minimization of the grand potential

$$\Omega[\rho] = \mathcal{F}_{\text{id}}[\rho] + \mathcal{F}_{\text{ex}}[\rho] - \int d\mathbf{r} \int d\sigma \mu_0(\sigma) \rho(\mathbf{r}, \sigma), \quad (\text{A.4})$$

$$\beta \mathcal{F}_{\text{id}}[\rho] = \int d\mathbf{r} \int d\sigma \rho(\mathbf{r}, \sigma) \{ \ln(\mathcal{V}(\sigma) \rho(\mathbf{r}, \sigma)) - 1 \}, \quad (\text{A.5})$$

(where $\mathcal{F}_{\text{id}}[\rho]$ is the ideal part of the DF while $\mu_0(\sigma)$ is the fixed chemical potential of species with length σ and $\mathcal{V}(\sigma)$ is the thermal volume of species with length σ) with respect to $\rho(\mathbf{r}, \sigma)$ gives us

$$\rho(\mathbf{r}, \sigma) = \rho_0(\sigma) \exp \left\{ -\frac{\delta \beta \mathcal{F}_{\text{ex}}}{\delta \rho(\mathbf{r}, \sigma)} + \beta \mu_0^{\text{ex}}(\sigma) \right\}, \quad (\text{A.6})$$

$\beta \mu_0^{\text{ex}}(\sigma) \equiv \beta \mu_0(\sigma) - \ln(\mathcal{V}(\sigma) \rho_0(\sigma))$ being the excess chemical potential of species with length σ . Near the bifurcation point, expanding the exponential around $\rho_0(\sigma)$ we obtain an integral equation for the perturbation $\epsilon(\mathbf{r}, \sigma)$

$$\epsilon(\mathbf{r}, \sigma) - \rho_0(\sigma) \int d\mathbf{r}' \int d\sigma' c^{(n)}(\mathbf{r}, \sigma, \sigma') \epsilon(\mathbf{r}', \sigma') = 0, \quad (\text{A.7})$$

where $c^{(n)}(\mathbf{r}, \sigma, \sigma')$ is the direct correlation function of the polydisperse mixture. The Fourier transform of Eq. (A.7) for the wave vector $\mathbf{q} = q(1, \dots, 0)$ give us

$$\hat{\epsilon}(q, \sigma) - \rho_0 h(\sigma) \int d\sigma' \hat{c}^{(n)}(q, \sigma, \sigma') \hat{\epsilon}(q, \sigma') = 0. \quad (\text{A.8})$$

The function $\hat{c}^{(n)}(q, \sigma, \sigma')$ can be obtained from (6) by replacing σ_i and σ_j by σ and σ' respectively. We define the functions

$$\epsilon_i^{(k)}(q) = \int d\sigma \sigma^i u_k(q\sigma/2) \hat{\epsilon}(q, \sigma), \quad k = 0, 1, \quad (\text{A.9})$$

where we have used the notation $u_0(q\sigma/2) = \cos(q\sigma/2)$, and $u_1(q\sigma/2) = 2 \sin(q\sigma/2)/q$. Inserting $\hat{c}^{(n)}(q, \sigma, \sigma')$ from equation (6) into equation (A.8), integrating over σ' , multiplying the result by $\sigma^l u_k(q\sigma/2)$ ($k = 0, 1$) and integrating again over σ we obtain the following linear system with respect to the functions $\epsilon_i^{(k)}(q)$:

$$\epsilon_l^{(k)}(q) + \rho_0 \sum_{i=0}^{n-1} \left(\mathcal{T}_{li}^{(k,0)}(q) \epsilon_i^{(0)}(q) + \mathcal{T}_{li}^{(k,1)}(q) \epsilon_i^{(1)}(q) \right) = 0, \quad (\text{A.10})$$

where we have defined the matrix coefficients

$$\mathcal{T}_{li}^{(k,0)}(q) = C_i^{n-1} \sum_{j=0}^i C_j^i \zeta_j m_{n+j+l-i-1}^{(k,1)}(q), \quad (\text{A.11})$$

$$\mathcal{T}_{li}^{(k,1)}(q) = C_i^{n-1} \sum_{j=0}^i C_j^i \left[\zeta_j m_{n+j+l-i-1}^{(k,0)}(q) + \zeta_{j+1} m_{n+j+l-i-1}^{(k,1)}(q) \right]. \quad (\text{A.12})$$

and the generalized moments

$$m_i^{(l,n)}(q) = \int d\sigma h(\sigma) \sigma^i u_l(q\sigma/2) u_n(q\sigma/2). \quad (\text{A.13})$$

The functions $\zeta_i(\xi_n, \dots, \xi_{n-i})$ are obtained from the same recurrence relations (7) with $\xi_i = \rho_0 \langle \sigma^i \rangle$ defined now through the moments of the distribution functions.

The system (A.10) can be put in the matrix form

$$\mathcal{M}(\rho_0, q) \begin{pmatrix} \boldsymbol{\epsilon}^{(0)}(q) \\ \boldsymbol{\epsilon}^{(1)}(q) \end{pmatrix} = \mathbf{0}, \quad (\text{A.14})$$

with

$$\mathcal{M}(\rho_0, q) = I + \rho_0 \begin{pmatrix} \mathcal{T}^{(0,0)}(q) & \mathcal{T}^{(0,1)}(q) \\ \mathcal{T}^{(1,0)}(q) & \mathcal{T}^{(1,1)}(q) \end{pmatrix}, \quad \boldsymbol{\epsilon}^{(k)} = \left(\epsilon_0^{(k)}, \dots, \epsilon_{n-1}^{(k)} \right)^T, \quad (\text{A.15})$$

and I the $2n \times 2n$ unitary matrix. The existence of a nontrivial solution of Eq. (A.14) give us the following set of equations

$$M(\rho_0, q) = \frac{\partial M}{\partial q}(\rho_0, q) = 0, \quad (\text{A.16})$$

(where we have defined $M(\rho_0, q) = \det[\mathcal{M}(\rho_0, q)]$) to find the values of ρ_0^* and q^* (the absolute minimum of $M(\rho_0, q)$ with respect to q) at bifurcation.

References

- [1] van Roij R, Mulder B and Dijkstra M, 1998 *Physica A* **261** 374
- [2] Wensink H H, Vroege G J and Lekkerkerker H N W, 2001 *J. Chem. Phys.* **115** 7319
- [3] Dubois S and Perera A, 2002 *J. Chem. Phys.* **116** 6354
- [4] Varga S, Galindo A and Jackson G, 2002 *J. Chem. Phys.* **117** 7207
- [5] Schmidt M and Denton A R, 2002 *Phys. Rev. E* **65** 021508
- [6] Martínez-Ratón Y, Velasco E and Mederos L, 2005 *Phys. Rev. E* **72** 031703; de las Heras D, Martínez-Ratón Y and Velasco E, 2007 *Phys. Rev. E* **76** 031704
- [7] Kranendonk W G T and Frenkel D, 1991 *Mol. Phys.* **72** 679; 1989 *J. Phys.: Condens. Matter* **1** 7735
- [8] Dijkstra M, van Roij R and Evans R, 1998 *Phys. Rev. Lett.* **81** 2268; 1998 *Phys. Rev. E* **59** 5744
- [9] Almarza N G and Enciso E, 1998 *Phys. Rev. E* **59** 4426
- [10] Martínez-Ratón Y and Cuesta J A, 1999 *J. Chem. Phys.* **111** 317
- [11] Lafuente L and Cuesta J A, 2002 *Phys. Rev. Lett.* **89** 145701
- [12] Widom B and Rowlinson J S, 1970 *J. Chem. Phys.* **52** 1670; Dickman R and Stell G, 1995 *J. Chem. Phys.* **102** 8674; Brader J M and Vink R L C, 2007 *J. Phys.: Condens. Matter* **19** 036101; Schmidt M, 2004 *J. Phys.: Condens. Matter* **16** L351; Santos A, López de Haro M and Yuste S B, 2010 *J. Chem. Phys.* **132** 204506; Dijkstra M, 1998 *Phys. Rev. E* **58** 7523
- [13] Conway J H and Sloane N J A, 1999 *Sphere Packings, Lattices, and Groups*, Springer, NY; Cohn H and Elkies N, 2003 *Ann. Math.* **157** 689; Cohn H, 2002 *Geom. Topol.* **6** 329
- [14] van Meel J A, Frenkel D and Charbonneau P, 2009 *Phys. Rev. E* **79** 030201 (R)
- [15] Skoge M, Donev A, Stillinger F H and Torquato S, 2006 *Phys. Rev. E* **74** 041127
- [16] Estrada C D and Robles M, 2010 *arXiv:1002.3407v3 cond-mat.soft*
- [17] Finken R, Schmidt M and Löwen H, 2001 *Phys. Rev. E* **65** 016108
- [18] Robles M and López de Haro M, 2007 *J. Chem. Phys.* **126** 016101
- [19] Bishop M and Whitlock P A, 2006 *J. Stat. Phys.* **126** 299; Lue L, Bishop M and Whitlock P, 2010 *J. Chem. Phys.* **132** 104509
- [20] Rohrmann R D and Santos A, 2007 *Phys. Rev. E* **76** 051202
- [21] Yuste S B, Santos A and López de Haro M, 2000 *Europhys. Lett.* **52** 158
- [22] Lafuente L and Cuesta J A, 2002 *J. Phys.: Condens. Matter* **14** 12079
- [23] Cuesta J A and Martínez-Ratón Y, 1997 *Phys. Rev. Lett.* **78** 3681; 1997 *J. Chem. Phys.* **107** 6379
- [24] Tarazona P, 2000 *Phys. Rev. Lett.* **84** 694
- [25] Buhot A and Krauth W, 1999 *Phys. Rev. E* **59** 2939
- [26] Lafuente L and Cuesta J A, 2005 *J. Phys. A: Math. Gen.* **38** 7461; 2004 *Phys. Rev. Lett.* **93** 130603
- [27] Tarazona P, Cuesta J A and Martínez-Ratón Y, 2008 *Lect. Notes Phys.* **753** 247
- [28] Jagla E A, 1998 *Phys. Rev. E* **58** 4701
- [29] Groh B and Mulder B, 2001 *J. Chem. Phys.* **114** 3653
- [30] Hoover W G, Hoover C G and Bannerman M N, 2009 *J. Stat. Phys.* **136** 715
- [31] Hoover W G and de Rocco A G, 1962 *J. Chem. Phys.* **36** 3141; Hoover W G and Poirier J C , 1963 *J. Chem. Phys.* **38** 327
- [32] van Swol F and Woodcock L V, 1987 *Mol. Simul.* **1** 95
- [33] Kirkpatrick T R, 1986 *J. Chem. Phys.* **85** 3515
- [34] Martínez-Ratón Y and Cuesta J A, 1998 *Phys. Rev. E* **58** R4080